Molecular Crystals and Liquid Crystals

ISSN: 1542-1406 (Print) 1563-5287 (Online) Journal homepage: http://www.tandfonline.com/loi/gmcl20

Simulation and electrical characterization of InN/ InP diodes

B. Hadjadj, Z. Benamara, N. Zougagh & B. Akkal

To cite this article: B. Hadjadj, Z. Benamara, N. Zougagh & B. Akkal (2016) Simulation and electrical characterization of InN/InP diodes, Molecular Crystals and Liquid Crystals, 627:1, 74-81, DOI: 10.1080/15421406.2015.1137147

To link to this article: http://dx.doi.org/10.1080/15421406.2015.1137147

Published online: 13 May 2016.

Submit your article to this journal

Article views: 30

View related articles

View Crossmark data

Full Terms & Conditions of access and use can be found at
http://www.tandfonline.com/action/journalInformation?journalCode=gmcl20

Download by: [College of Business Education] **Date:** 22 December 2016, At: 12:24

MOL. CRYST. LIQ. CRYST.
2016, VOL. 627, 74–81
http://dx.doi.org/10.1080/15421406.2015.1137147

Taylor & Francis
Taylor & Francis Group

Simulation and electrical characterization of InN/InP diodes

B. Hadjadj, Z. Benamara, N. Zougagh, and B. Akkal

Laboratoire de Microélectronique Appliquée, Département d'électronique, Université Djillali Liabès de Sidi Bel Abbés, Sidi Bel Abbés, Algérie

ABSTRACT
Fabrication and electrical characterization of thin films obtained by the nitridation of InP (100) substrates in a Glow Discharge Source (GDS) are presented and discussed. The electrical parameters of InN/InP Schottky diode such as the saturation current (I_s), barrier height (ϕ_b), ideality factor (n) and series resistance (R_s) were determined. These parameters were calculated using the current-voltage (I–V) characteristics and are compared with those obtained by an analytical model. This model was used in order to identify the transport phenomena. Semi-log forward I-V, Cheung functions and Norde methods were used in order to determine the series resistance R_s. The measured values of I_s, (ϕ_b), and n for the studied sample are of 1.33×10^{-4} A cm^{-2}, 0.46 eV and 3.31, respectively.

KEYWORDS
InN/InP flms; nitrudation; electrical characterization; simulation

1. Introduction

The III nitrides, such as InN attract a growing interest in recent years because they exhibit interesting properties for nanoelectronics and optoelectronics, such as the direct gap and high electron mobility. They exhibit a refractory nature which allows to consider their application in hostile conditions, high temperature, high electric power or high frequency.

However, the development of these III-nitrides, has encountered an obstacle that is the lack of suitable substrates for their growth because of the importance of the lattice mismatch between the parameters of elements and III nitrides. The totality of the available substrates leads to the formation of high density of defects in the material. The semiconductor substrates III/V such as InP are potentially interesting materials for the growth of InN. However, the characteristics of the resulting Schottky diodes, are closely related to the surface and interface states.

We have elaborated the Au/InN/InP diodes using a glow discharge source (GDS) and characterized them for their electric properties. Then, we have plotted current versus bias voltage and extracted a electronical parameters (saturation current (Is), ideality factor (n), Schottky barrier height ϕ_b). We have also developped a simulation program plotting the current-voltage characteristic I (V) of a InN/InP Schottky diode. It allows us to identify the transport phenomena in these devices. The work is completed with determination of serie resistance using different methods as semi-log forward I–V, Cheung functions and Norde's one.

CONTACT B. Hadjadj br80h@yahoo.fr Laboratoire de Microélectronique Appliquée, Département d'électronique, Université Djillali Liabès de Sidi Bel Abbés, 22000 Sidi Bel Abbés, Algérie
Color versions of one or more of the figures in the article can be found online at www.tandfonline.com/gmcl.
© 2016 Taylor & Francis Group, LLC

2. Experimental part

The InN thin films were prepared by the nitridation of InP substrates using a glow discharge source (GDS) in ultra high vacuum. The InP (1 0 0) wafers used in the present work, were doped with carrier concentration of 10^{16} cm^{-3}. They were chemically cleaned in ultrasonic bath before introduction in the ultra-high vacuum chamber (10^{-6} to 10^{-7} Pa). After the introduction into the chamber, a low amount of carbon and oxygen contamination was detected. These impurities were removed by *in situ* cleaning with low energy Ar^+ ions (300 eV), and current density of 2 μA cm^{-2} [1, 7] The ion bombardment cleaning is a key step for the first nitridation process, since it creates at the surface metallic indium droplets in well-controlled quantities (mean coverage: 25%, mean height: 4 atomic monolayers). The nitriding of the InP samples was carried out by the plasma type source for discharging (glow discharge source (GDS)), to create one or two monolayers of InN on InP(100) substrates through the consumption of indium droplets by nitrogen atoms. In this kind of nitrogen source a continuous plasma is produced by the applied high voltage (about 2.2 kV). In each nitridation, the sample was kept under a nitrogen flow (grazing flow) for 30 min, below the InP substrate decomposition temperature of about 350°C. The obtained InN layers were 4 monolayers thick. To realize a metallic gate a molybdenum mask used. This mask allows performing electrical measurements with a gold gate of diameter ≈ 1 mm and thick layers of about 1000 Å. Hence, zones with and without deposition were created. It made possible subsequent studies of surface homogeneity and deposits cleanliness possible. We noted that the current–voltage $I(V)$ characteristic measurements were made through a standard set-up (two 616 electrometer).

3. Results and discussion

3.1. *Experimental results and discussion*

Figure 1 presents evolution of current versus bias voltage. The current flow through a Schottky contact can be described by the well-known thermionic emission (TE) theory. The I–V

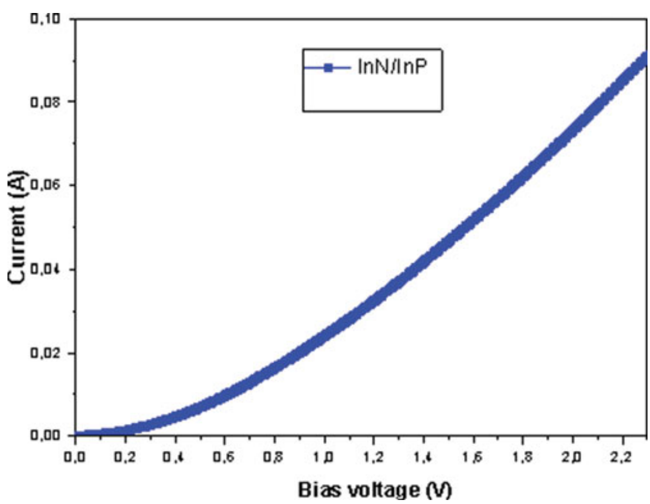

Figure 1. Plots of *I–V* data characteristics for Au/InN/InP Schottky diode.

relationship for Schottky diodes is given by [1,2].

$$I = I_s\left[\exp\left(\frac{qV}{nkT}\right) - 1\right] \tag{1}$$

where n is the ideality factor, q is the electronic charge, k is the Boltzmann constant, T is absolute temperature in Kelvin, V is the applied voltage and I_s is the saturation current given by:

$$I_s = SA^*T^2\exp\left(\frac{-q\Phi_b}{kT}\right) \tag{2}$$

The quantities S and ϕ_b are the Schottky contact area (785×10^{-5} cm^{-2}), the zero bias apparent barrier height (BH), respectively. A^* is the effective Richardson constant and was theoretically calculated as [3].

$$A^* = \frac{4\pi m^*qk^2}{h^3} = \frac{m^*}{m_0}120 \quad Acm^{-2}K^{-2} \tag{3}$$

For n-type InP substrate, the electron effective mass is $0.078m_0$ as given by Palic et al. [4]. Putting it into Eq. (3) one gets $A^* = 9.4A/cm^2\ K^2$.

On the other hand, the barrier height ϕ_b can be calculated from I_o using the following equation:

$$\Phi_b = \frac{kT}{q}\ln\left(\frac{SA^*T^2}{I_0}\right) \tag{4}$$

Accprding to Eq. (1), the ideality factor n can be written as:

$$n = \frac{q}{kT}\left(\frac{dV}{d(\ln I)}\right) \tag{5}$$

The plots of I–V data characteristics for Au/InN/InP Schottky diode are shifted to higher bias-voltage with increasing voltage. The forward bias current for the sample is 0.02 A at applied voltage less than 1V.

In similar a work Petit et al. [6], studied the effect the incidence angle of the nitrogen flow on electrical characteristics of Hg/InN/InP Schottky diodes synthesis using a glow discharge source (GDS). They have found that the forward bias current density between 1.68 and 3,36 V is lower than 0.0122 A and equal to 0.0355 A at the normal nitrogen flow (0°) and grazing (80°) nitrogen flows, respectively.

Figure 2 illustrated typical $\ln[I/1 - e^{-\frac{qV}{kT}}]$ versus V characteristic of Au/InN/InP Schottky diode at room temperature for the sample. This curve shows two linear regions separated by a transition segment, the slope and the intercept of this plot on the current axis allows to determine the ideality factor n and the saturation current I_s evaluated to 3.31 and 1.33×10^{-4} A.cm^{-2}, respectively. By substituting the values of Is in Eq. (4), we have deduced the height of the potential barrier ϕ_b which is equal to 0.46 V. These values are very interesting and are comparable with the values reported by Talbi et al. [7]. Benamara et al. [8] have studied Au/ /heated InSb /InP Schottky diode with barrier height value of 0.624 eV and ideality factor value of 1.61. The barrier height value of 0.624 eV that they have obtained for the Au//heated InSb/InP device due to InN interlayer is remarkably higher than that achieved with conventional metal/semiconductor contacts such as Au/InP diode, whose barrier height was 0.441 eV.

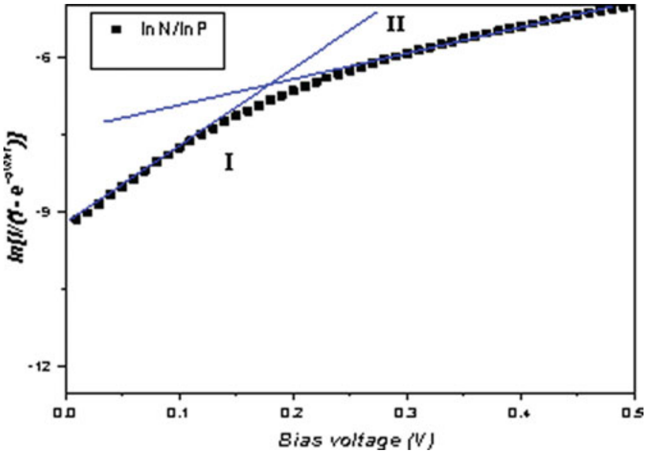

Figure 2. Plots of $\ln[I/1 - e^{-\frac{qV}{kT}}]$ versus V characteristic of Au/InN/InP Schottky diode at room temperature.

The series resistance (R_s) is an important parameter for the electrical characteristics of the Schottky barrier diodes. Various methods were suggested how to determine the effect of series resistance on electrical parameters of devices. Fig. 2 shows clearly, for higher polarization voltages, the change in the slope of the $\ln[I/1 - e^{-\frac{qV}{kT}}]$ characteristic caused by the series resistance R_s. By using these approximation and analyzing region II, we have estimated the value of the series resistance R_s to be equal to 25 Ω.

This result is better than the value of series resistance obtained by Akkal et al. [10]. In this work, the series resistance is equal to 85 Ω under dark and decreases to 67 Ω under illumination.

The series resistance R_s were also calculated using a method developed by Cheung and Cheung [11] and confirmed by Werner [12]. Cheung's functions can be written as follows:

$$\frac{dV}{d(\ln I)} = \frac{nkT}{q} + IR_s \tag{6}$$

$$H(I) = V - \left(\frac{nkT}{q}\right)\ln\left(\frac{I}{SA^*T^2}\right) = n\Phi_b + IR_s \tag{7}$$

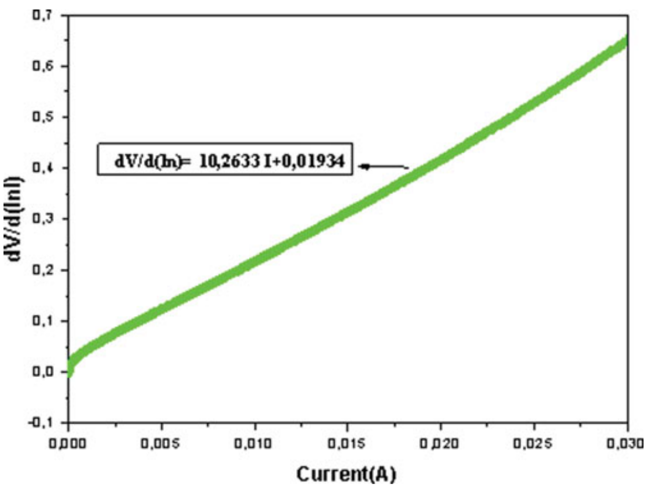

Figure 3. Experimental dependence dV/dln(I) vs. I.

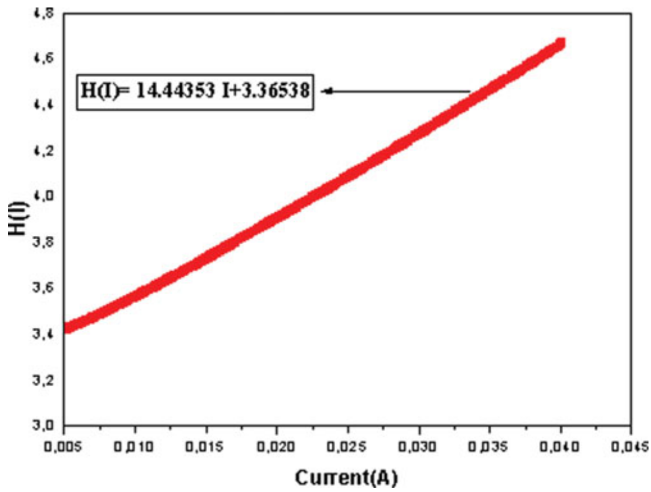

Figure 4. Experimental dependence *H*(*I*) vs. *I*.

Eq. (6) gives a straight line the data in the downward curvature region of the forward bias I–V characteristics. The term IR_s is the voltage drop across the series resistance of Schottky diode. In Fig. 3 and Fig. 4, the experimental dV/dln(I) *vs* I and $H(I)$ *vs* I plots are presented. Thus, the slope and y-axis intercept of the plot $dV/d\ln(I)$ *vs* I give R_s and nkT/q, respectively. The plot of $H(I)$ *vs* I (Fig. 4), according to Eq. (7), gives a straight line with the y-axis intercept equal to $n\,\phi_{b0}$. The slope of this plot also provides the second determination of R_s which can be used to check the consistency of Cheung's approach.

Norde's method was also used to calculated the series resistance R_s of the Au/InN/InP Schottky structure. The method involves a modified Norde function, $F(V)$, being plotted against voltage $F(V)$, as given by [13].

$$F(V) = \frac{V}{\gamma} - \frac{kT}{q}\ln\left(\frac{I(V)}{SA^{*}T^{2}}\right) \tag{8}$$

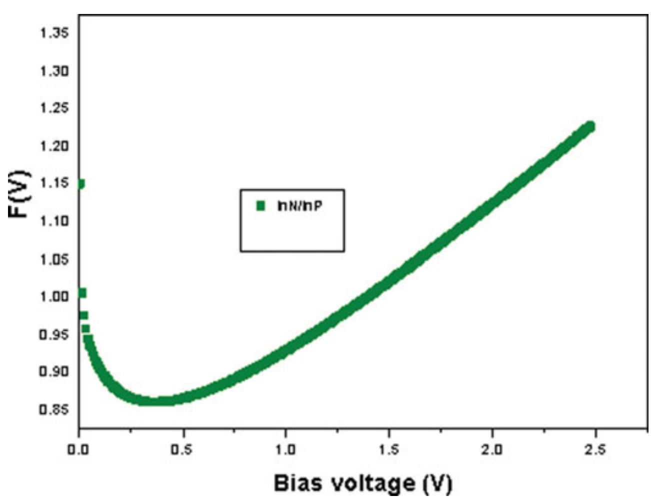

Figure 5. Plot of *F*(*V*) versus *V*.

Table 1. The values of series resistance obtained using different methods.

	Semi-log forward I-V	Cheung functions		Norde's function
	$Ln[I/(1\text{-}e^{qV/kT})]$ vs V	dV/d(lnI)	H(I)	F(V)
(Rs)	25 Ω	10.26 Ω	14.44 Ω	9.14 Ω

where γ is a dimensionless integer having value greater than the ideality factor and $I(V)$ is the current obtained from the I–V curve. The barrier height of the Au/InN/InP diode structure can be obtained using the following equation:

$$\Phi_b = F'(V_0) + \frac{V_0}{\gamma} - \frac{kT}{q} \tag{9}$$

where $F(V_{\min})$ is the minimum value of $F(V)$ of the plot of $F(V)$ *versus* V, and $V_{\min}$ is the corresponding voltage. Fig. 5 shows the plots of $F(V)$ *versus* V for the studied sample.

The series resistance can be estimated from the Norde's function and is given by

$$R_s = \frac{kT(\gamma - n)}{qI_0} \tag{10}$$

Table 1 presents the results of series resistance measurements, obtained by semi-log forward I-V, Cheung functions and Norde's methods. The values were calculated using Eqs. (6) and (7). Those obtained from the semi-log forward I–V method are larger than when using the Cheung functions and Norde's method.

3.2. *Results and discussions*

The analytical model current in Schottky diodes, based on the thermoelectric emission (TE) theory, is given by the following equations [14,15]:

$$I = I_0\left(1 - \frac{V_d}{V}\right)\left[\exp\left(\frac{q(V - R_s)}{nkT}\right) - 1\right] \tag{11}$$

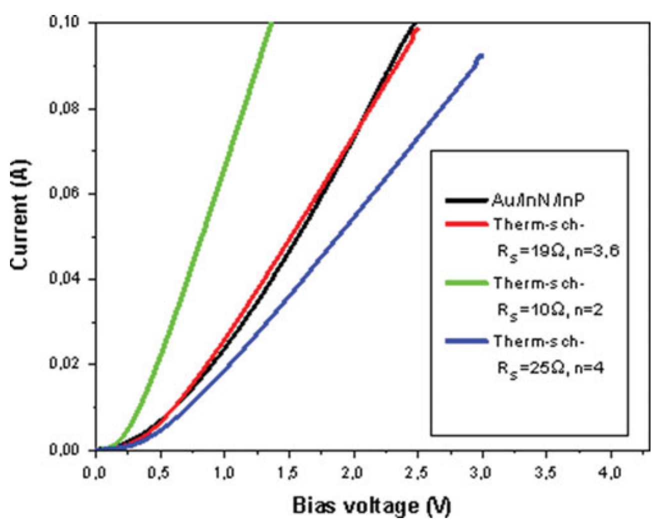

Figure 6. Comparison of experimental curve with the calculated ones (with different values of R_s and n).

Table 2. Results obtained from the characteristics I (V) of InN/InP.

Sample	I_s (A)	N	R_s (Ω)	ϕ_b (V)	V_d (V)
Au/InN/InP	1.33×10^{-4}	3.31	25	0.46	0.34
Au/InP (simulated)	1.58×10^{-4}	3.6	19	0.42	0.30

$$I_0 = \frac{SqA^*V_d}{k} \exp\left(-\frac{qV_d}{nkT}\right) \tag{12}$$

$$V_d = \frac{kT}{q} \ln\left[\frac{N_{d(InN)}N_{c(InP)}}{N_{d(InP)}N_{C(InN)}}\right] + \frac{\Delta E_c}{q} \tag{13}$$

Using these equations, we have plotted the current versus bias voltage characteristics for different electrical parameters (ideality factor n, series resistance R_s, ...) (see figure 6). In this figures the obtained curves are compared with the experimental ones. We see that the characteristic of a Schottky diode approaches the experimental curve and are similar to the I-V curve with $R_s = 19\ \Omega$ and $n = 3.6$. In that case the calculated curve is identical with the experimental one.

These results confirm that our structure is a Shottky diode and the conduction phenomenon can be ascribed as a thermoionic emission. The values of series resistance, ideality factor, barrier height and diffusion potential are similar to those obtained by the semi-log forward I-V method (see Table 2).

4. Conclusions

In this paper we have reported the results of electrical characterization of Au/InN/InP Schottky junctions. The studied structure is realized using the glow discharge source (GDS). From have plotted the current *vs* bias voltage dependence the electrical parameters: I_s, ϕ_b and n were determined. They were found to be equal to 1.33×10^{-4} A cm^{-2}, 0.46 eV and 3.31, respectively.

The current *versus* bias voltage dependence was calculated theoretically. The comparison simulation of the experimental and calculated curves allowed us to identify the transport phenomena behind the thermionic emission (TE).

The series resistance was calculated using different methods. The values of series resistance dependences: $\mathrm{Ln}[I/(1-e^{qV/kT})]$ *vs* V, $[R_s(dn/d(InI))R_sH(I))]$ and $R_s(F(V)$, calculated from Cheung's function [dn/(d(In),H(I)] and Norde's function F(H) appeared to be different. However, we show clearly that the result obtained by using the $\mathrm{Ln}[I/(1-e^{qV/kT})]$vs V method is comparable with the simulated values.

References

[1] Akkal, B., Benamaraa, Z., Bideux, L., & Gruzza, B. (1999). *Microelect. J.*, *30*, 673–678.

[2] Talbi, A., Benamara, M. A., Benamara, Z., Akkal, B., Gruzza, B., Bideux, L., Robert, C., & Monier, G. (2013). *J. Optoelectr. Adv. Mat.*, *15*(5–6), 509–513.

[3] Akkal, B., Benamara, Z., Abid, H., Talbi, A., & Gruzza, B. (2004). *Mater. Chem. Phys.*, *85*, 27–31.

[4] Palic, E. D., & Wallis, R. F. (1961). *Phys. Rev.*, *123*, 131–134.

[5] Ameur, K., Benamara, Z., Mazari, H., Benseddik, N., Khelifi, R., Mostefaoui, M., Benamara, M. A., Gruzza, B., Bluet, J.M., & Bru-Chevallier, C. (2014). *Sensors & Transducers*, *27*, 9–14.

[6] Petit, M., Robert-Goumet, Ch., Bideux, L., Gruzza, B., Benamara, Z., Bachir Bouiadjra, N., & Matolin, V. (2004). *Appl. Surf. Sci.*, *234*, 451–456.
[7] Talbi, Z., Benamara, A., Akkal, B., Gruzza, B., Bideux, L., Robert, C., Varenne, C., & Chami, N. (2006). *Mater. Sci. Eng. A*, *437*, 254–258.
[8] Benamara, Z., Akkal, B., Talbi, A., Gruzza, B., & Bideux, L. (2002). *Mater. Sci. Eng. C*, *21*, 287–290.
[9] Chawanda, A. (2010). *J. Korean Phy. Soc.*, *57*, 1970–1975.
[10] Akkal, B., Benamara, Z., Bachir Bouiadjra, N., Tizi, S., & Gruzza, B. (2006). *Appl. Surf. Sci.*, *253*, 1065–1070.
[11] Cheung, S.K., & Cheung, N.W. (1986). *Appl. Phys. Lett.*, *49*, 85.
[12] Werner, J.H. (1988). *Appl. Phys. A, 47*, 291.
[13] Norde, H. (1979). *J. Appl. Phys.*, *50*, 5052–5053.
[14] Marty, A., Bailbe, J. P., & Rey, G. (1982). *Revue Phys. Appl.*, *17*, 453–464.
[15] Ahmetoglu (Afrailov), M. (2008). *Thin Solid Films*, *516*, 1227–1231.